Wind Gyres

Here we derive the simplest (and oldest; Stommel, 1948) theory to explain western boundary currents like the Gulf Stream, and then discuss the relation of the theory to more realistic gyres. This expands the material in the lecture slides in circulation.pdf.

Recall several relations from the lecture on Equations. The depth-integrated horizontal transport $\mathbf{T}$ is non-divergent and can be represented with a transport streamfunction Ψ,

$$\mathbf{T} \;=\; \hat{\mathbf{z}} \times \nabla_h \Psi \,.$$

The depth-integrated steady vorticity balance, including contributions from Coriolis force and Ekman layer Reynolds stress divergence, is

$$\beta \partial_x \Psi \;=\; \frac{1}{\rho_0} \operatorname{curl}[\tau^s - \tau^b] \,. \tag{1}$$

We choose the simple, linear bottom stress law derived by linear Ekman theory with constant κ_v, *viz.,*

$$\tau^b \;=\; \rho_0 R^b \mathbf{u}_i^b \,, \tag{2}$$

where R^b [m s^{-1}] is a bottom drag coefficient, and we assume the interior currents are wholly barotropic, $\mathbf{u}_i^b = \mathbf{T}/h$. Thus,

$$\frac{1}{\rho_0}\, \tau^b \;=\; R \overline{\mathbf{u}} \;=\; \frac{R}{h} \mathbf{T} \,.$$

Thus, if h is spatially uniform (*i.e.,* the bottom is flat),

$$\frac{1}{\rho_0} \operatorname{curl}[\tau^b] \;=\; \frac{R}{h} \nabla^2 \Psi \,,$$

and we can state the horizontal boundary-value problem for Ψ as

$$\begin{aligned} \frac{R}{h} \nabla^2 \Psi + \beta \partial_x \Psi \;&=\; \frac{1}{\rho_0} \operatorname{curl}[\tau^s] \,, \\ \text{with} \quad \Psi \;&=\; 0 \quad \text{on the boundary.} \end{aligned} \tag{3}$$

The boundary condition assures no flow through the horizontal boundary. This is a 2D, second-order, elliptic PDE for $\Psi(x,y)$ given the time-mean wind stress $\tau^s(x,y)$.

We already saw a partial solution of this model in the Sverdrup relation DE(33):

$$\Psi^{Sv}(x,y) \;=\; -\frac{1}{\beta \rho_0} \int_x^{x_e(y)} \operatorname{curl}[\tau^s]\, dx \,, \tag{4}$$

where $x_e(y)$ is the location of the eastern boundary. This balances the right-side forcing in (3) with the first left-side term. It also satisfies the boundary condition at the eastern boundary x_e but not at the western boundary $x_w(y)$ because

$$\Psi_w^{Sv}(y) \;=\; -\frac{1}{\beta \rho_0} \int_{x_w(y)}^{x_e(y)} \operatorname{curl}[\tau^s]\, dx$$

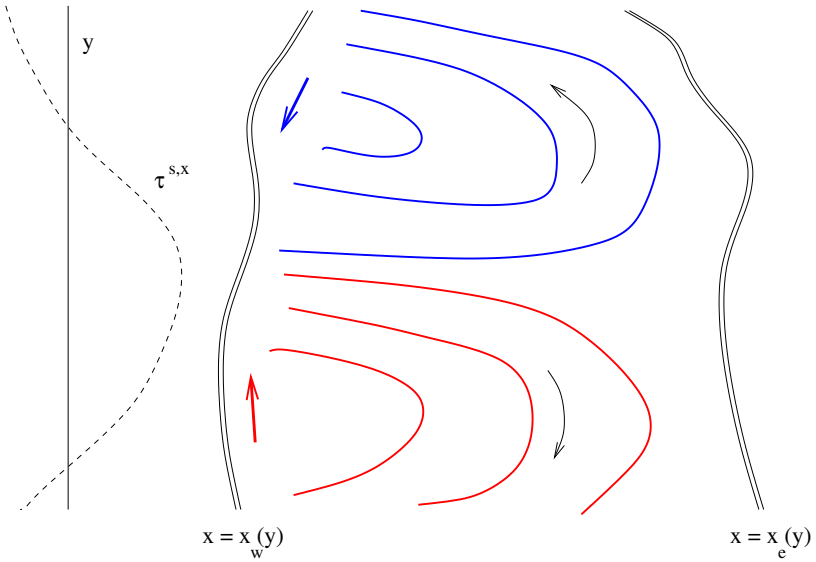

Figure 1: Sketch of Sverdrup gyres in the Northern-Hemisphere. A zonal surface stress profile is on the left, with a maximum westerly wind at middle latitudes. The associated Sverdrup transport streamfunction $\Psi^{Sv}(x, y)$ from (4) is on the right in an oceanic basin bounded on the west and east by x_w and x_e. Flow is along isolines of Ψ as indicated by the arrows. The subpolar gyre has $\Psi^{Sv} < 0$ (blue contours) and counterclockwise circulation due to the positive wind curl, $-\partial_y \tau^{s,x} > 0$, at high latitudes. The subtropical gyre has $\Psi^{Sv} > 0$ (red contours) and clockwise circulation due to the negative wind curl, $-\partial_y \tau^{s,x} < 0$, in middle latitudes. The flow near the western boundary is not sketched because it does not satisfy the Sverdrup balance. However, by transport non-divergence within a bounded basin, there must be return flow for steady-state mass balance; these occur in western boundary currents (WBCs) as indicated by the colored arrows. This is a repeated figure.

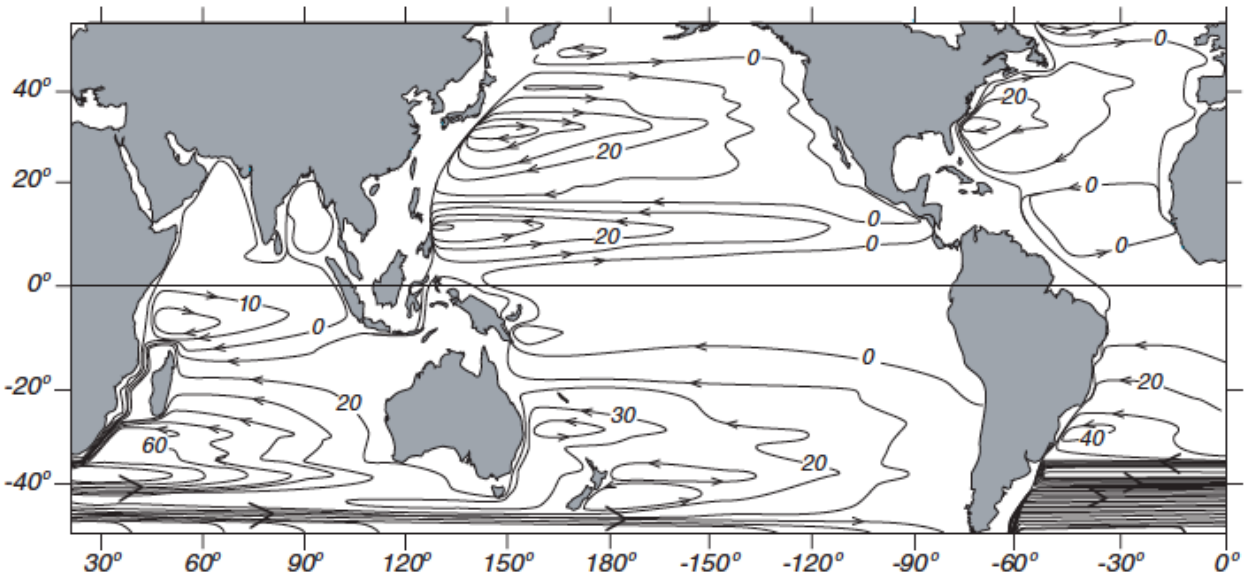

Figure 2: Global Sverdrup transport Ψ^{Sv} [Sv] calculated with (4) using the observed mean wind. Notice the subtropical and near-equatorial gyres, the subpolar gyres in the north (partly off the page), and the approach to the Antarctic Circumpolar region without zonal boundaries. (Stewart, 2008)

is usually nonzero.

The Sverdrup transport $\Psi^{Sv}(x,y)$ is sketched in Fig. 1 and diagnosed from the global mean wind field in Fig. 2.

To complete the solution of (3) we add a correction component, *i.e.,*

$$\Psi \;=\; \Psi^{Sv} + \Psi^{w}\,, \tag{5}$$

where after substitution the boundary-value problem for the correction is

$$\begin{aligned} \nabla^2\Psi^w + \frac{h\beta}{R}\partial_x\Psi^w \;&=\; -\,\nabla^2\Psi^{Sv}\,, \\ \text{with}\quad \Psi^w \;&=\; -\,\Psi^{Sv} \quad \text{on the boundary.} \end{aligned} \tag{6}$$

Define $L^w \;=\; R/h\beta$, which has the unit of length. For oceanic conditions,

$$L^w \;\ll\; L^d\,,$$

where L^d is the scale of the basin and/or the mean wind field. By (4) L^d is also the scale for Ψ^{Sv} in both x and y. If we posit that L^w is the appropriate zonal scale for Ψ^w and that Ψ^{Sv}_w is the appropriate amplitude scale for both Ψ components, then we can make scale estimates for the second-derivative terms in (6):

$$\partial_x^2\Psi^w \;\sim\; \frac{\Psi^{Sv}_w}{L^{w\,2}} \quad\gg\quad \partial_y^2\Psi^w \;\text{and}\nabla^2\Psi^{Sv} \;\sim\; \frac{\Psi^{Sv}_w}{L^{d\,2}}\,.$$

Thus, we can approximate the full $\Psi^w(x,y)$ problem by a simpler boundary-layer problem in x (independently for each value of y):

$$\begin{aligned} \partial_x^2\Psi^w + \frac{1}{L^w}\,\partial_x\Psi^w \;&=\; 0\,, \\ \Psi^w(x_w) \;=\; -\,\Psi^{Sv}_w \qquad &\text{and} \quad \Psi^w(x_e) \;=\; 0\,. \end{aligned} \tag{7}$$

This is a second-order ODE in x, so it has two homogeneous solutions. We can factor this ODE operator into $[\partial_x - 1/L^w]$ times $\partial_x]$; the first factor has is exponential function of x decaying to the east, and the second is a constant in x. The general solution is their linear combination with coefficients c_1 and c_2:

$$\Psi^w \;= c_1\, e^{-x/L^w} + c_2\,.$$

The coefficients are determined by the boundary conditions. Because $x_w < x_e$ and $L^w \ll L^d$, $e^{-x_e/L^w} \;\ll\; e^{-x_w/L^w}$; so $c_2 \approx 0$ and $c_1 \approx -\,\Psi^{Sv}_w e^{x_w/L^w}$. Thus, the solution to (6) is

$$\Psi(x,y) \;\approx\; -\,\Psi^{Sv}_w e^{-(x-x_w)/L^w} + \Psi^{Sv}\,. \tag{8}$$

For further simplicity we now assume τ^s is independent of x and identify L^d with $x_e - x_w$. So,

$$\Psi(x,y) \;=\; \frac{\mathrm{curl}[\tau^s]}{\beta\rho_0}\,\left(\,L_d e^{-(x-x_w)/L^w} - L^d + x - x_w\,\right)\,, \tag{9}$$

and the associated meridional barotropic velocity is

$$\overline{v}(x) \;=\; \frac{1}{h}\partial_x\Psi \;=\; \frac{\mathrm{curl}[\tau^s]}{h\beta\rho_0}\,\left(1 - \frac{L^d}{L^w}e^{-(x-x_w)/L^w}\right) \tag{10}$$

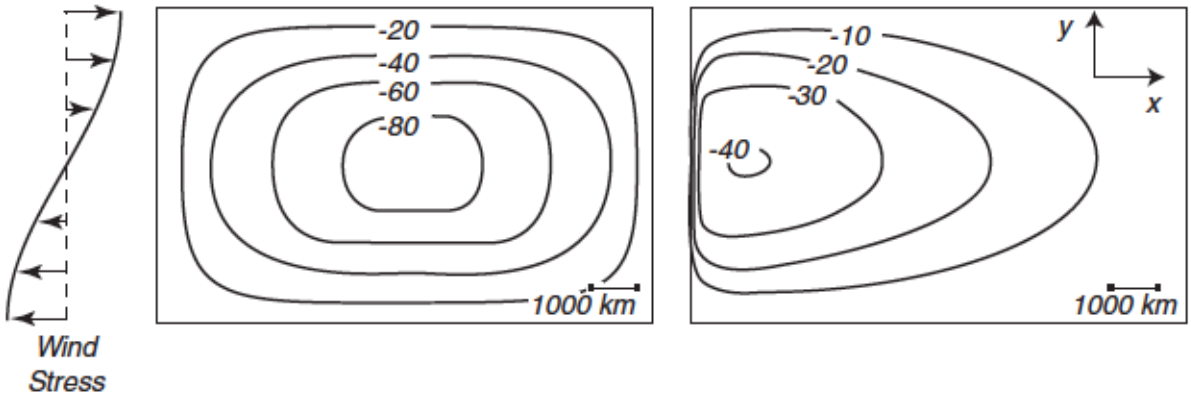

Figure 3: The transport streamfunction Ψ [Sv] for a subtropical gyre in a closed domain. (Here it is plotted with the wrong sign; Ψ is a maximum in the middle of an anticyclonic gyre in the Northern Hemisphere). The wind stress $\tau^x(y)$ is on the left, and the solution to (6) is on the right. The value of R is empirically chosen to match the width L^w ($\sim$ 100 km) of the Gulf Stream along the east coast of North America. For comparison the middle panel shows a solution to (3) except that β is set to zero (*i.e.,* a f-plane model). In this case the interior flow is not Sverdrup flow and there is no WBC. (Stewart, 2008)

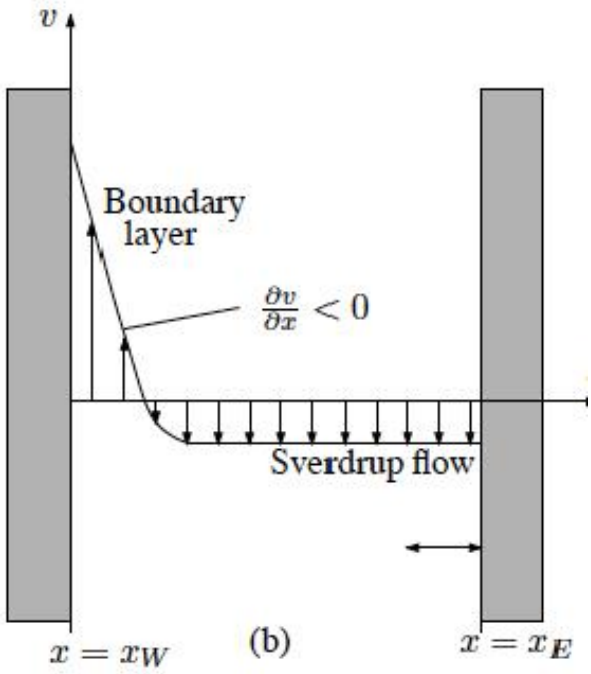

Figure 4: Sketch of the barotropic meridional velocity $\overline{v}(x)$ across a subtropical gyre with curl$[\boldsymbol{\tau}^s] < 0$. The interior velocity is a southward Sverdrup flow and the narrow western boundary current (WBC) is much faster. The zonally integrated meridional transport $\int T^y\, dx$, is zero; *i.e.,* the WBC provides an equal and opposite mass flux to the Sverdrup flow.

(Figs. 3-4).

We derived (9) assuming in anticipation that $\Psi^{Sv}_{x_e} = 0$ in (4). Had we instead retained the possibility of a "constant"-of-integration for (1), *i.e.,* $\Psi^{Sv}_e(y) \neq 0$, then we would have derived that $c_2 = -\Psi^{Sv}_e(y)$, leading to the same outcome in (9).

The reason the boundary current is on the western side is that the exponential homogeneous solution, e^{-x/L^w}, is decaying toward the east, *i.e.,* $L^w = R/h\beta$ is a positive number. This is because β is positive on Earth ($\mathbf{\Omega}$ is counter-clockwise rotation about the North pole)) and because R is positive since the stationary sea bed provides a drag on the adjacent currents, not *vice versa*. Of course, $h > 0$ by definition. A WBC exists because $\beta \neq 0$ (*cf.,* Fig. 3) and because turbulence mix mean momentum; in this model the relevant mixing occurs within the bottom Ekman layer as $\overline{\mathbf{u}'w'}$. Notice that this mixing effect is only quantitatively significant in our solution within the WBC, even though it is acting everywhere in (3).

A more mechanistic explanation for why the western boundary current is on the western side comes from taking the area integral of (3) over the whole basin. The β term integrates to zero since

$$\int\int dx\, dy\, \partial_x \Psi \;=\; \int dy\, \Psi\Big|^{x_e}_{x_w} \;=\; 0\,.$$

The integral of the bottom drag term is proportional to the barotropic circulation C by application of Stokes integral theorem,

$$\frac{1}{h}\int\int dx\, dy\, \nabla^2\Psi \;=\; \int\int dx\, dy\, \hat{\mathbf{z}}\cdot\nabla\times\overline{\mathbf{u}} \;=\; \oint ds\, \overline{\mathbf{u}}\cdot\hat{\mathbf{s}} \;\equiv\; C\,,$$

where $\hat{\mathbf{s}}$ is unit vector traversing the boundary in a counter-clockwise direction and ds is its differential arc length. Thus, the circulation balance from (3) is

$$C \;=\; \frac{1}{\rho_0 R}\int\int dx\, dy\, \mathrm{curl}[\tau^s]\,, \tag{11}$$

and this is negative in a subtropical gyre. Hence, $C < 0$, and the integrated boundary current must be in a clockwise direction. This is true for $\overline{v}$ in Fig. 4 with the boundary current on the west. A hypothetical northward flow boundary current on the east, while consistent with overall mass balance by opposing the southward Sverdrup flow, would not be consistent with circulation balance (11). Thus, a negative vorticity input by the wind in the subtropical gyre, leading to downward Ekman pumping and southward Sverdrup transport, also requires an anticyclonic gyre circulation with a northward WBC.

Now we lift our eyes from the narrow perspective of this simple theory to makes some more general remarks on oceanic wind-driven gyres.

- There are other simple models for a wind gyre that show the same overall structure of an interior Sverdrup flow and a WBC. One alternative is to assume that horizontal turbulence provides the important mixing in the WBC region, *i.e.,* $\overline{u'v'}$ in momentum and $\overline{u'\zeta^{z\,\prime}}$ in vorticity. This turbulence would mesoscale or submesoscale eddies rather than bottom boundary-layer turbulent eddies.

- Obviously, many generalizations are needed before this simple model can be realistically complete. The principal missing effects here are pycnocline density stratification and associated buoyancy forcing and baroclinic circulation, time-variability in $\tau^{\mathbf{s}}$, nonlinear advection

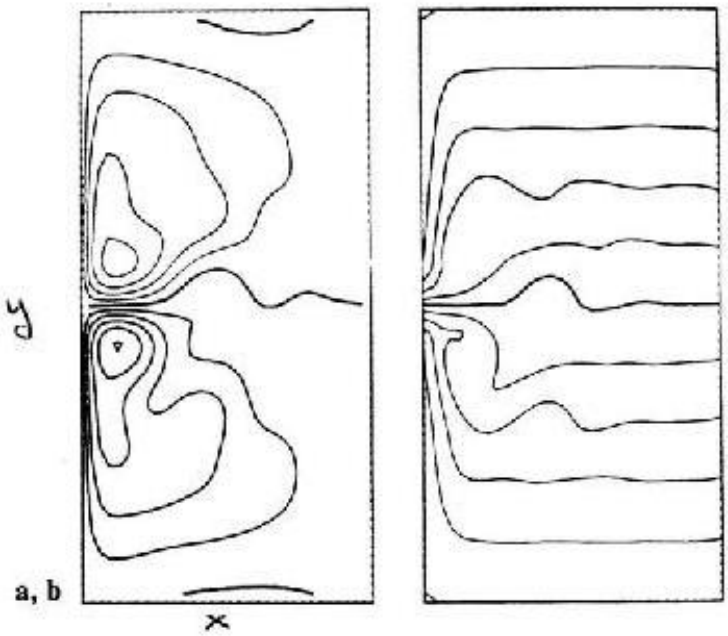

Figure 5: Time averaged $\overline{\psi}$ (left) and $\overline{Q}_{qg} = \overline{\zeta}^{w} + \beta y$ (right) from a nonlinear, QG, barotropic model with steady, "double gyre" wind stress (*i.e.,* $\tau^{s\,x}(y)$ is maximum in the center). The averaged circulation is unstable, mesoscale eddies arise, and the eddy term $\overline{J[\psi', Q'_{qg}]}$ allows $\overline{\psi}$ to deviate from the Sverdrup flow in the interior recirculation zone. (Marshall, 1984)

by the circulation, and mean circulation barotropic and baroclinic instabilities that generate mesoscale eddies which in turn provide momentum and buoyancy mixing that reshape the circulation. A modestly less simple model — but one requiring a computer for solution — includes the latter two effects in the barotropic QG equations with steady wind forcing (Fig 5). By comparison with Fig. 3) we see two main differences: the WBC only separates in a narrow eastward jet rather than in a broad interval along the western boundary, and there is a region of enhanced recirculation (*i.e.,* larger than the total Sverdrup transport) in the corner of the gyre next to the separated jet.

- Wind-gyre circulation is essentially geostrophic outside the Ekman layers. Thus, it is reflected in the surface dynamic height field (Fig. 6) where the extrema are usually close to the western boundary as in our simple solution just interiorward of the WBC. (The Antarctic Circumpolar Current [ACC] is the biggest exception.) We see some pattern similarities with Ψ^{Sv} in Fig. 2. We can approximately identify $\overline{\eta}$ with $f\Psi/gh_{pyc\,0}$. The relevant depth here is the pycnocline depth h_{pyc} since real gyres are baroclinic and have most of their wind-driven transport in the upper ocean and weak flow in the abyss. The latter implies that

$$g\overline{\eta} \;\approx\; g'(\overline{h}_{pyc} - h_{pyc\,0})\,,$$

where $g' = g\Delta\rho/\rho_0$ is gravity reduced by the relative stratification in the pycnocline; *i.e.,* the pycnocline is deeper where the sea surface elevation is higher such that the horizontal pressure gradient force is weak in the abyss. Some numbers: $\Psi = 30$ Sv (3×10^7 m^3 s^{-1}); $f = 10^{-4}$ s^{-1}; $g = 10$ m s^{-2}; $\Delta\rho/\rho_0 = 2.5 \times 10^{-3}$; $\overline{\eta} = 0.7$ m; and $\overline{h}_{pyc} - h_{pyc\,0} = 300$ m.

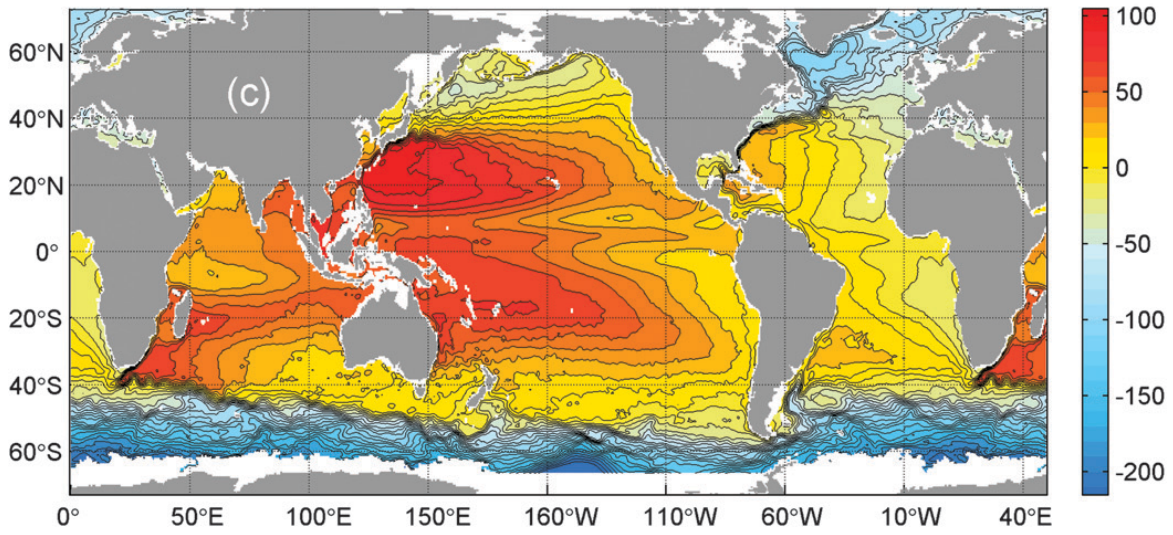

Figure 6: Global mean sea-level relative to an iso-surface of Earth's gravitational potential (*i.e.,* dynamic height) [in m with contour interval 0.1 m]. It is an analysis from altimetry and surface drifters for the period 1993-2002. This figure is repeated.

- Real gyres are dynamically complex, with stratification, baroclinicity, and eddy mixing all playing essential roles (*e.g.,* Figs. 7-8). Analytic theories have some skill in representing these influences, but computational general circulation models (GCMs) are necessary to adequately simulate them.

References

Marshall, J., 1984: Eddy-mean-flow interaction in a barotropic ocean model. *Q. J. Roy. Met. Soc.* **110**, 573-590.

Stewart, Robert, 2008: *Introduction To Physical Oceanography.* `http://oceanworld.tamu.edu/resources/ocng_textbook/PDF_files/book_pdf_files.html`

Stommel, H., 1948: The westward intensification of wind-driven ocean currents. *Trans. Amer. Geophys. Union* **29**, 202-206.

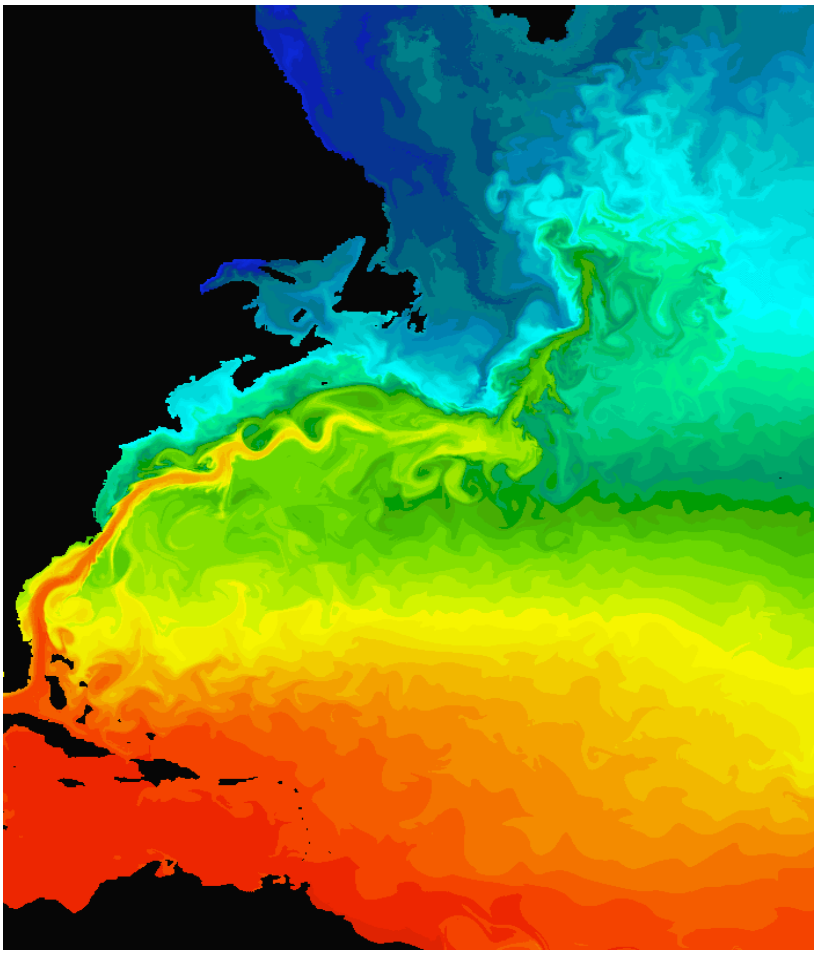

Figure 7: Instantaneous of SST in the Western North Atlantic. The warm, narrow, separated Gulf Stream and mesoscale eddies are evident. This figure is repeated.

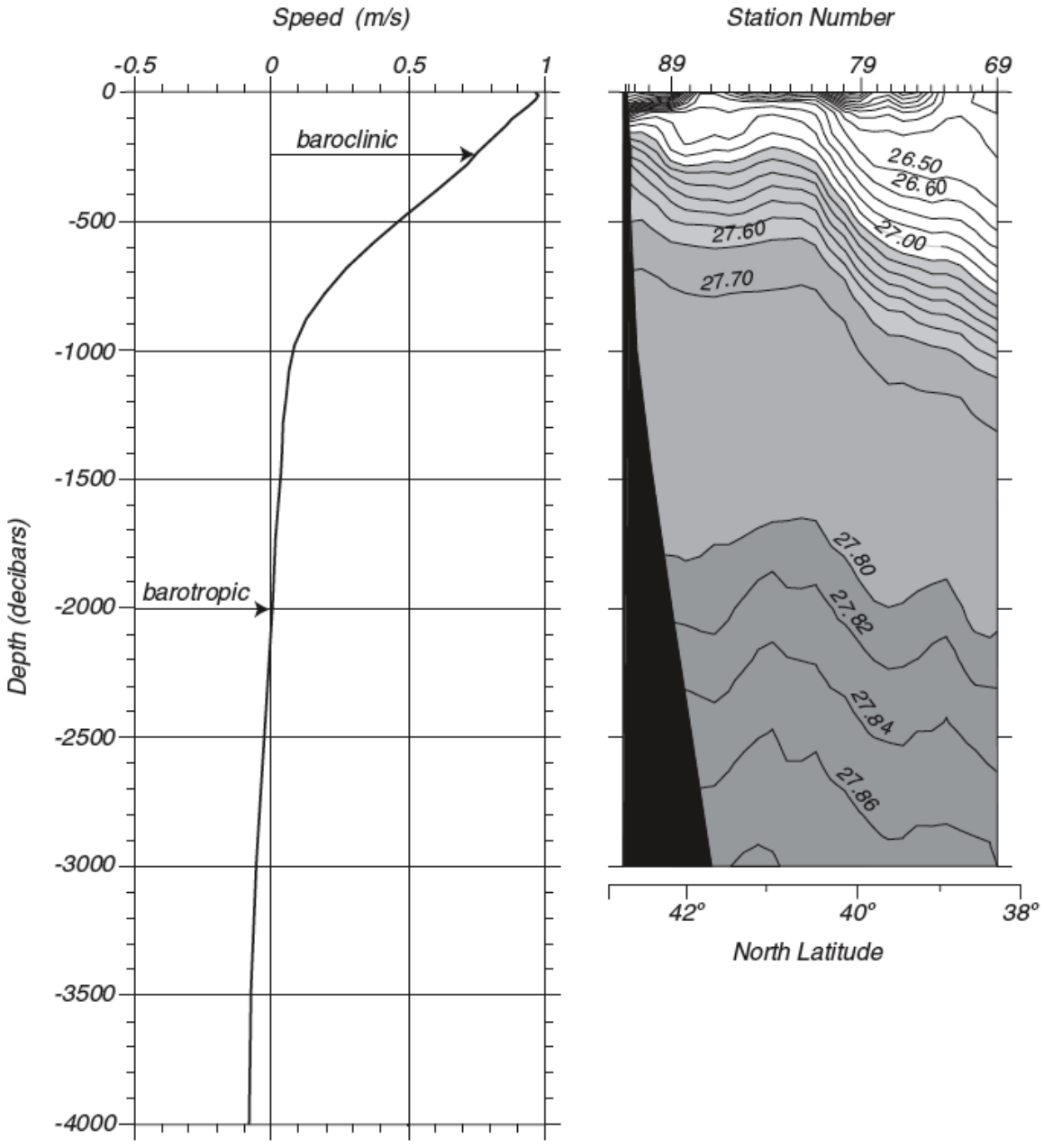

Figure 8: Meridional section of density ($\sigma = \rho - 10^3$ kg m^{-3}) from hydrographic stations taken across the Gulf Stream downstream from its separation point on the western boundary (right) and the vertical profile of the geostrophic zonal current [m s^{-1}] at its center (left). Notice that the gyre circulation is baroclinic, with the strong currents in and above the main pycnocline, rather than with a barotropic vertical profile. (Stewart, 2008)